Biochemistry

pubs.acs.org/biochemistry Article

Shorter Alkanesulfonate Carbon Chains Destabilize the Active Site Architecture of SsuD for Desulfonation

Shruti Somai,[§] Kun Yue,[§] Orlando Acevedo, and Holly R. Ellis*

Cite This: *Biochemistry* 2023, 62, 85−94 Read Online

ACCESS | Metrics & More | Article Recommendations | Supporting Information

ABSTRACT: Bacteria have evolved to utilize alternative organosulfur sources when sulfur is limiting. The SsuE/SsuD and MsuE/MsuD enzymes expressed when sulfur sources are restricted, are responsible for providing specific bacteria with sulfur in the form of alkanesulfonates. In this study, we evaluated why two structurally and functionally similar $FMNH_2$-dependent monooxygenase enzymes (MsuD and SsuD) are needed for the acquisition of alkanesulfonates in some bacteria. In desulfonation assays, MsuD was able to utilize the entire range of alkanesulfonates (C1−C10). However, SsuD was not able to utilize smaller alkanesulfonate substrates. Interestingly, SsuD had a similar binding affinity for methanesulfonate (MES) (15 ± 1 μM) as MsuD (12 ± 1 μM) even though SsuD was not able to catalyze the desulfonation of the MES substrate. SsuD and MsuD showed decreased proteolytic susceptibility in the presence of $FMNH_2$ with MES and octanesulfonate (OCS). Tighter loop closure was observed for the MsuD/$FMNH_2$ complex with MES and OCS compared to SsuD under comparable conditions. Analysis of the SsuD/$FMNH_2$/MES structure using accelerated molecular dynamics simulations found three different conformations for MES, demonstrating the instability of the bound structure. Even when MES was bound in a similar fashion to OCS within the active site, the smaller alkane chain resulted in a shift of $FMNH_2$ so that it was no longer in a position to catalyze the desulfonation of MES. The active site of SsuD requires a longer alkane chain to maintain the appropriate architecture for desulfonation.

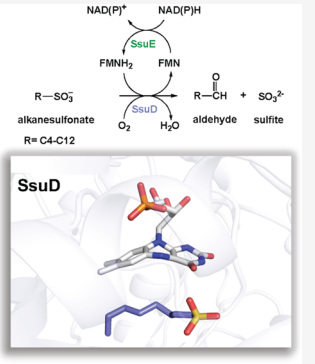

INTRODUCTION

Sulfur plays a key role in diverse metabolic processes that occur in all organisms. Bacteria predominantly rely on inorganic sulfate or cysteine as their main sulfur sources.[1,2] However, due to the limited availability of inorganic sulfate in many environments, bacteria need to utilize alternative sulfur sources to obtain this critical element. During sulfur starvation, bacteria can express specific proteins that provide an alternative means of obtaining sulfur through organosulfur uptake, sulfur acquisition from organic compounds, and protection against reactive oxygen species (ROS).[1−3] The type of alternative sulfur source utilized by bacteria is not universal and varies between bacterial groups. *Escherichia coli* (*E. coli*) expresses enzymes during sulfur starvation that catalyze the desulfonation of taurine (TauD) and alkanesulfonates (SsuE/SsuD) as sulfur sources. *Pseudomonas aeruginosa* (*P. aeruginosa*) has a complex system for sulfur acquisition due to its presence in diverse environments and is able to utilize alkanesulfonates, sulfate esters, and aromatic sulfonates as sulfur sources.[1,4−6] In addition to the alkanesulfonate monooxygenase system, *P. aeruginosa* also contains a methanesulfonate monooxygenase system (MsuE/MsuD) that allows the organism to utilize a broad range of alkanesulfonate (C1−C12) substrates for sulfur acquisition.[5] Both the alkanesulfonate and methanesulfonate monooxygenase systems belong to the group C flavin monooxygenases that consist of a flavin reductase and a separate $FMNH_2$-dependent monooxygenase to catalyze the desulfonation reaction.[7,8]

SsuD from *E. coli* and MsuD from *P. aeruginosa* share ∼60% amino acid sequence identity and have a similar active site architecture (Figure 1A,B).[9] Both monooxygenases are TIM-barrel proteins that contain a dynamic loop region near their active site that is located at the C-terminal end of the β barrel.[9−11] This dynamic loop region is found in different bacterial SsuD and MsuD enzymes and is proposed to close over the active site with the ordered binding of reduced flavin and the alkanesulfonate. Loop closure over the active site would exclude the bulk solvent and stabilize reactive intermediates that are formed during catalysis, as well as prevent the premature release of any intermediates and bound substrates.[12,13] Previous studies provided evidence that SsuD was protected from proteolysis in the presence of $FMNH_2$, suggesting that $FMNH_2$ binding promotes partial loop closure over the active site.[10,11,14] For MsuD, $FMNH_2$ binding organizes the active site for the binding of the sulfonated

Received: October 13, 2022
Revised: December 2, 2022
Published: December 19, 2022

https://doi.org/10.1021/acs.biochem.2c00586
Biochemistry 2023, 62, 85−94

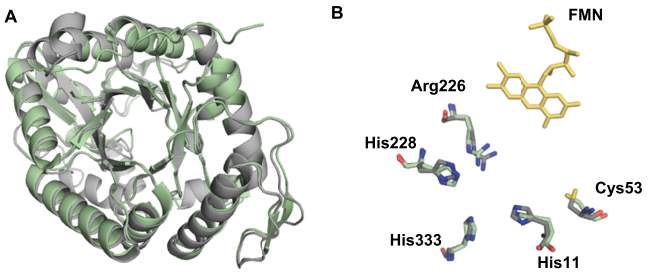

Figure 1. Structural comparison of SsuD and MsuD. (A) Overlay of SsuD (green) and MsuD (gray). Both proteins have a TIM-barrel fold and similar insertional regions that diverge from the classic TIM-barrel structure. The MsuD structure was generated with AlphaFold.[15] The C-terminal region (356−381) showed low confidence and was not included in the structure. (B) Active site of SsuD (green) and MsuD (gray). The numbering of active site amino acids is for the SsuD structure. The flavin highlighted is bound in the MsuD structure. PDB: 1M41.

substrate.[10] The binding of methanesulfonate (MES) initiates a second conformational change that fully encloses the active site.

Although both monooxygenases have a similar active site arrangement, SsuD from *E. coli* has reduced relative activity with MES.[16] MsuD from *P. aeruginosa* showed a clear preference for MES monitoring relative activity, while the MsuD homolog from *Pseudomonas fluorescens* (*P. fluorescens*) showed a broader alkanesulfonate range with a higher relative activity observed for octanesulfonate (OCS).[5,10] The substrate preferences provide a wide range of alternative alkanesulfonate substrates for bacteria that are susceptible to limiting sulfur conditions. Given the similarity of the active site structure, it is unclear what contributes to the substrate specificity of SsuD and MsuD. Differences in the dynamic loop that closes over the active site may contribute to the specificity, and recent studies suggest that the C-terminal region is also involved in substrate recognition.[10] These studies directly compare the substrate specificity and conformational changes that occur with the binding of substrates to SsuD and MsuD. Complementary kinetic analyses and accelerated molecular dynamics (aMD) simulations were performed to establish how enzymes with similar active sites are able to both recognize and discern between similar substrates.

MATERIALS AND METHODS

Materials. All chemicals for protein purification and enzyme assays were purchased from Sigma-Aldrich, Fischer, Bio-Rad, or Fluka.

Expression and Purification of Recombinant Proteins. SsuD, SsuE, MsuD, and MsuE enzymes were purified as described previously.[17,18] The concentrations of SsuD and SsuE proteins were determined from A_{280} measurements using molar extinction coefficients of 47.9 and 20.3 mM^{-1} cm^{-1}, respectively. The concentrations of MsuD and MsuE proteins were determined from A_{280} measurements using molar extinction coefficients of 49.4 and 7.54 mM^{-1} cm^{-1}, respectively.[17,18]

Steady-State Kinetic Analyses. A coupled assay monitoring sulfite production was used to determine the steady-state kinetic parameters of SsuD and MsuD. The reactions were initiated with the addition of NADPH (500 μM) into a reaction mixture containing MsuD or SsuD (0.2 μM), MsuE or SsuE (0.6 μM), FMN (2 μM), and varying concentrations of the sulfonated substrates (0−1000 μM) in 25 mM Tris−HCl (pH 7.5) and 0.1 M NaCl at 25 °C. The reaction was quenched after 3 min with 8 M urea followed by the addition of DTNB (1 mM). After the addition of DTNB, the reaction was allowed to develop at room temperature for 2 min, and the absorbance was measured at 412 nm using a molar extinction coefficient for the TNB anion of 14.1 M^{-1} cm^{-1}. All assays were performed in triplicate, and the steady-state kinetic parameters were determined by fitting the data to the Michaelis−Menten equation.

Spectrofluorometric Titrations. The affinity of SsuD and MsuD for oxidized flavin was monitored by spectrofluorometric titration. The binding of FMN to SsuD and MsuD (0.5 μM) was performed under aerobic conditions by adding aliquots of oxidized flavin (5−100 μM) to the enzyme solution in a fluorescence cuvette. Spectral changes were monitored at 344 nm (excitation at 280 nm) after each addition of FMN following a 2 min incubation.

For the titration of reduced flavin, an anaerobic solution of SsuD and MsuD (0.5 μM) in 25 mM potassium phosphate (pH 7.5) and 100 mM NaCl (1.0 mL total volume) was titrated with a solution of $FMNH_2$. The enzyme solution was transferred inside the glovebox and treated with glucose (10 mM) and glucose oxidase (0.1 μM) to remove trace amounts of oxygen after which it was diluted in anaerobic 25 mM potassium phosphate (pH 7.5) and 100 mM NaCl buffer. The buffer was made anaerobic by bubbling with ultrahigh-purity argon gas for 1 h before being transferred inside the anaerobic glovebox. Reduced flavin was prepared in 25 mM potassium phosphate (pH 8.0), 20 mM EDTA, and 100 mM NaCl. The flavin solution was bubbled with ultrahigh-purity argon gas for 30 min before being transferred to the anaerobic glovebox. After the addition of glucose (10 mM) and glucose oxidase (0.1 μM) to both protein and flavin, the solutions were incubated in an anaerobic glovebox for 2 h to remove trace amounts of dioxygen. The anaerobic flavin solution was photoreduced inside a gastight titrating syringe with a long-wavelength UV lamp, after which the anaerobic cuvette was assembled inside the anaerobic glovebox. SsuD or MsuD was titrated with 15 aliquots of $FMNH_2$ (0.08−1.2 μM). The fluorescence spectrum at 344 nm (excitation at 280 nm) was recorded following a 2 min incubation after each addition of reduced flavin. Bound $FMNH_2$ was determined using eq 1.

$$[FMNH_2]_{bound} = [E]\frac{I_0 - I_c}{I_0 - I_f} \quad (1)$$

where $[FMNH_2]_{bound}$ represents the concentration of the $FMNH_2$-bound enzyme. [E] represents the initial concentration of the enzyme, I_0 is the initial fluorescence intensity of the enzyme prior to the addition of the substrate, I_c is the fluorescence intensity of the enzyme following each addition, and I_f is the final fluorescence intensity. The concentration of $FMNH_2$ bound was plotted against the free substrate to obtain the dissociation constant (K_d) according to eq 2.

$$Y = \frac{B_{max}X}{K_d + X} \quad (2)$$

where Y and X represent the concentration of bound and free substrates, respectively, following each addition. B_{max} is the maximum binding at equilibrium with the maximum concentration of substrate.

https://doi.org/10.1021/acs.biochem.2c00586
Biochemistry 2023, 62, 85−94

The affinity of $FMNH_2$-bound SsuD and MsuD for sulfonated substrates was investigated by a similar fluorometric titration method employed for reduced flavin binding. The sulfonated substrates were transferred inside the glovebox and dissolved in 25 mM potassium phosphate (pH 7.5) and 100 mM NaCl buffer that was made anaerobic as described. The buffer was made anaerobic by bubbling with ultrahigh-purity argon gas for 1 h before being transferred inside the anaerobic glovebox. Aliquots of an anaerobic solution of the sulfonated substrates (2.5−50 μM) in an airtight titrating syringe were added to an anaerobic solution of either SsuD or MsuD (1.0 μM) and $FMNH_2$ (2.0 μM) in 25 mM potassium phosphate (pH 7.5) and 100 mM NaCl (1.0 mL total volume). Reduced flavin was prepared as described but was added to the titration cuvette with the enzymes prior to the assembly of the anaerobic titration syringe containing the sulfonated substrates.

Limited Proteolytic Analysis. The susceptibility of SsuD and MsuD to proteolysis was investigated with trypsin in the absence and presence of FMN. Trypsin stock solution (1 mg/mL) was prepared in 1 mM HCl/1 mM $CaCl_2$ (pH 8.4). Samples of SsuD or MsuD (15 μM) were prepared in 200 mM ammonium bicarbonate/1 mM $CaCl_2$ (pH 8.4) and treated with TPCK-treated trypsin (10 μg/mL). To monitor the effects of oxidized flavin on protein proteolytic susceptibility, FMN (20 μM) in 25 mM potassium phosphate (pH 7.5) and 10% glycerol was included. After the addition of trypsin, samples (10 μL) were taken at various times (15 s, 30 s, 45 s, 1 min, and 3 min) and quenched through heat denaturation for 2 min at 90 °C. The degree of proteolysis of each sample was analyzed by SDS-PAGE. The protein band was quantified with ImageJ software (NIH, Bethesda, MD) to determine the percent digestion.

To measure the degree of proteolysis in the presence of $FMNH_2$, an anaerobic solution of FMN (200 μM) was prepared in 25 mM potassium phosphate (pH 8.0), 20 mM EDTA, and 10% glycerol. The FMN solution was bubbled with ultrahigh-purity argon gas for 30 min before being transferred to an anaerobic chamber. The SsuD or MsuD solutions were prepared in a glovebox with 200 mM ammonium bicarbonate (pH 8.4) and 1 mM $CaCl_2$. The buffer was made anaerobic by bubbling with ultrahigh-purity argon gas for 1 h before being transferred inside the anaerobic glovebox. After the addition of glucose (10 mM) and glucose oxidase (0.1 μM), both the enzyme and FMN solution were incubated in an anaerobic glovebox to remove trace amounts of dioxygen. The $FMNH_2$ solution was photoreduced inside a gastight syringe with a long-wavelength UV lamp. The proteolytic susceptibility of SsuD and MsuD (15 μM) was also evaluated in the presence of $FMNH_2$ (20 μM) and the sulfonated substrate (200 μM). The sulfonated substrate was resuspended in anaerobic 25 mM potassium phosphate (pH 7.5) and 10% glycerol. The buffer was made anaerobic by bubbling with ultrahigh-purity argon gas for 1 h before being transferred inside the anaerobic glovebox. The reaction was started with the addition of trypsin, and samples (10 μL) were taken at various times (15 s, 30 s, 45 s, 1 min, and 3 min). The reaction was quenched through heat denaturation for 2 min at 90 °C after which the degree of proteolysis of each sample was analyzed by SDS-PAGE.

COMPUTATIONAL METHODS

Molecular Dynamics Simulation of SsuD and MsuD. To investigate the alkanesulfonate binding specificity of SsuD and MsuD, accelerated molecular dynamics (aMD) simulations were performed for (1) a methanesulfonate monooxygenase (MsuD) without substrates, (2) MsuD bound with reduced flavin ($FMNH_2$) and MES, and (3) an alkanesulfonate monooxygenase (SsuD) bound with $FMNH_2$ and MES.[19,20]

Enzyme Preparation. The Cartesian coordinates for the monomer MsuD structures from *Pseudomonas aeruginosa* were constructed using the I-TASSER online server with the protein sequence (Scheme S1 in the Supporting Information). The top 10 templates used by I-TASSER included the most recent crystal structure of MsuD from *P. fluorescens* (PDB ID 7JV3, released 2021-05-26).[10] The top model with the highest C score was utilized to carry out the current simulations. The SsuD model was taken from our previous aMD simulation effort, and details are provided in a prior publication.[21] The $FMNH_2$ ligand was inserted into the active site region of SsuD and MsuD based on a superposition with coordinates from previous SsuD simulation.[21] The MES was inserted into SsuD and MsuD using AutoDock Vina with a grid box that encompassed the proposed active site. Default flexible protocols of Vina using the Iterated Local Search global optimizer algorithm were utilized to perform the docking. The binding modes were set to 10, the exhaustiveness of the global search was set to 100, and a maximum energy difference between the best and the worst binding modes was set to 10 kcal/mol.

aMD Protocol. The coordinate and parameter files of SsuD and MsuD systems were generated using the leap module of the Amber16 package, where the appropriate hydrogen atoms were added.[22] The system was solvated with TIP3P water molecules using a box that extended to 10 Å beyond the enzyme.[23] Sodium ions were added to maintain system charge neutrality. The Amber force field was applied to construct the topology files for the protein, while the generalized Amber force field (GAFF) was used to generate the related parameters for the ligands.[24,25]

For each enzymatic complex, the initial structure was conjugate gradient (CG) minimized for 5000 steps for water molecules only followed by 10,000 steps of CG optimization for the entire system. After minimization, the system was slowly heated from 0 to 300 K using an NVT ensemble for 50 ps using the weak-coupling algorithm with a temperature coupling value of 2.8 ps. Then, the system was switched to an NPT ensemble at 300 K and 1 atm for 500 ps using a Berendsen barostat and the weak-coupling algorithm with a coupling value of 2.0 ps for both pressure and temperature. Next, the system was equilibrated for an additional 500 ps with an NVT ensemble. After this equilibration procedure, 10 ns of production data at NVT using unbiased MD was collected to derive the boost parameters needed for the subsequent aMD simulation using a best-practices procedure (Table S1 in the Supporting Information).[26] These aMD bias potentials allow the system to overcome high energy barriers and only require the evolution of a single copy of the system. The bias boost potential function, $V(r)$, which is a continuous positive value, is utilized whenever the potential value $V(r)$ gets below a certain chosen energy value E.[19] Finally, the aMD simulation was carried out in the NVT ensemble for 1000 ns. All MD simulations utilized the GPU-accelerated version of AMBER 16 featuring the particle mesh Ewald method to compute the long-range Coulomb force, periodic boundary conditions (PBC) with a nonbonded cutoff distance of 12 Å, and a time step of 1.0 fs.

https://doi.org/10.1021/acs.biochem.2c00586
Biochemistry 2023, 62, 85−94

Table 1. Steady-State Kinetic Parameters for SsuD and MsuD Using Sulfonated Substrates of Varying Carbon Lengths

SsuD	k_{cat} (s^{-1})	K_m($M \times 10^{-6}$)	k_{cat}/K_m (M^{-1} s^{-1}, $\times 10^4$)
methanesulfonate	—[a]	—	—
ethanesulfonate	—	—	—
butanesulfonate	0.56 ± 0.14	363 ± 193	0.15 ± 0.09
hexanesulfonate	1.20 ± 0.06	123 ± 17	0.98 ± 0.14
octanesulfonate	1.06 ± 0.04	62 ± 8	1.7 ± 0.23
decanesulfonate	1.01 ± 0.03	30 ± 4	3.4 ± 0.5
MsuD	k_{cat} (s^{-1})	K_m($M \times 10^{-6}$)	k_{cat}/K_m (M^{-1} s^{-1}, $\times 10^4$)
methanesulfonate	0.30 ± 0.01	36 ± 7	0.83 ± 0.16
ethanesulfonate	0.48 ± 0.09	275 ± 159	0.17 ± 0.10
butanesulfonate	0.30 ± 0.16	235 ± 200	0.13 ± 0.13
hexanesulfonate	0.64 ± 0.04	118 ± 20	0.54 ± 0.10
octanesulfonate	0.59 ± 0.02	49 ± 6	1.20 ± 0.15
decanesulfonate	0.47 ± 0.02	39 ± 5	1.21 ± 0.16

[a]Value could not be determined under the experimental conditions used.

Computational Analysis. Clustering, root-mean-square deviation (RMSD) calculations, and dihedral angle analysis were conducted using the ptraj and cpptraj programs within AmberTools.[27] For the clustering analysis, the average linkage algorithm was utilized. RMSD calculations were carried out by comparing backbone (N, C_α, and C) protein atoms and the distance deviations to the first frame over time.

RESULTS

Evaluating the Kinetic Parameters of Wild-Type SsuD and MsuD. Steady-state kinetic analyses monitoring sulfite production were performed to evaluate the range of alkanesulfonate carbon chain lengths utilized by SsuD and MsuD (Table 1 and Figures S1 and S2 in the Supporting Information). The kinetic parameters of SsuD have been evaluated with OCS based on the initial characterization of the enzyme, but the kinetic parameters have not been reported for alkanesulfonate substrates with varied carbon chain lengths. SsuD gave similar k_{cat}/K_m values with C6−C10 alkanesulfonates; however, no detectible sulfite production was observed with MES or ethanesulfonate (ETS). MsuD gave a k_{cat}/K_m value of 0.83 × 10^4 M^{-1} s^{-1} with MES, but the activity decreased with C2 and C4 sulfonate substrates. However, as the carbon length increased, the k_{cat}/K_m values were comparable to MES.

The differences in the kinetic parameters of SsuD and MsuD with methanesulfonate as a substrate suggested that there may be a difference in the binding affinity of each enzyme. Therefore, the binding affinities of SsuD and MsuD were evaluated through spectrofluorometric titration experiments using different sulfonated substrates. Binding studies with oxidized and reduced flavin to each enzyme were also performed to determine if the dissociation constants (K_d) for oxidized and reduced FMN to SsuD and MsuD were comparable (Table 2). Both SsuD and MsuD showed an ∼100-fold higher affinity for $FMNH_2$ compared to FMN (Figure S3 in the Supporting Information). The similar K_d values for MES and OCS suggest that both enzymes might utilize similar binding modes for reduced flavin (Figure S4 in the Supporting Information). Additionally, the absence of the SsuD activity with MES was not due to overt changes in the binding affinity, as SsuD had similar K_d values for MES and OCS. The K_d values obtained for MsuD with MES and OCS were comparable to SsuD.

Table 2. Dissociation Constants for SsuD and MsuD

	K_d, FMN ($M \times 10^{-6}$)	K_d, $FMNH_2$ ($M \times 10^{-6}$)	K_d, OCS ($M \times 10^{-6}$)	K_d, MES ($M \times 10^{-6}$)
SsuD	15 ± 2	0.19 ± 0.02	8.7 ± 0.7	15 ± 1
MsuD	15 ± 4	0.20 ± 0.03	7.2 ± 2.1	12 ± 1

Proteolytic Susceptibility of SsuD and MsuD. A mobile loop in the $FMNH_2$-dependent monooxygenases closes over the active site with the binding of substrates/products.[9−11,14,21] SsuD shows decreased proteolytic susceptibility in the presence of reduced flavin compared to FMN. The proteolytic sites cleaved first were located on the mobile loop, and the decrease in proteolysis was attributed to conformational changes of the mobile loop with the binding of reduced flavin.[11,14] The proteolytic susceptibility of MsuD was also evaluated in the presence of reduced flavin to determine if flavin binding reduced the proteolytic susceptibility. Digestion of MsuD quenched at various incubation times showed a decreased proteolytic susceptibility with reduced flavin compared to MsuD alone (Figure S5 in the Supporting Information). The proteolytic susceptibility of both enzymes was similar with 45 ± 4% of SsuD/$FMNH_2$ and 46 ± 5% of MsuD/$FMNH_2$ remaining after 180 s. There were more bands observed with MsuD/$FMNH_2$ compared to SsuD/$FMNH_2$ due to a greater number of basic amino acids (Figure S5 in the Supporting Information). Additionally, differences in the proteolytic susceptibility of MsuD and SsuD with $FMNH_2$ were evaluated in the presence of MES and OCS (Figure 2). Digestion of the SsuD/$FMNH_2$/OCS complex was similar to $FMNH_2$ only with 51 ± 7% undigested protein remaining (Figure 2A). Even though MES was not a substrate, SsuD showed similar proteolytic susceptibility in the presence of MES and $FMNH_2$ (53 ± 8% undigested) compared to $FMNH_2$/OCS (Figure 2B). These results further support the ability of SsuD/$FMNH_2$ to bind MES in an inactive ternary complex. While SsuD showed a similar proteolytic susceptibility with $FMNH_2$ alone or with $FMNH_2$/alkanesulfonates, MsuD demonstrated altered proteolysis under comparable conditions. There was a decrease in the proteolytic susceptibility of MsuD/$FMNH_2$/MES (64 ± 10% undigested) and MsuD/$FMNH_2$/OCS (66 ± 12% undigested) compared to the MsuD/$FMNH_2$ complex only, suggesting that MsuD is in an altered conformation with both reduced flavin and alkanesulfonates bound.

https://doi.org/10.1021/acs.biochem.2c00586
Biochemistry 2023, 62, 85−94

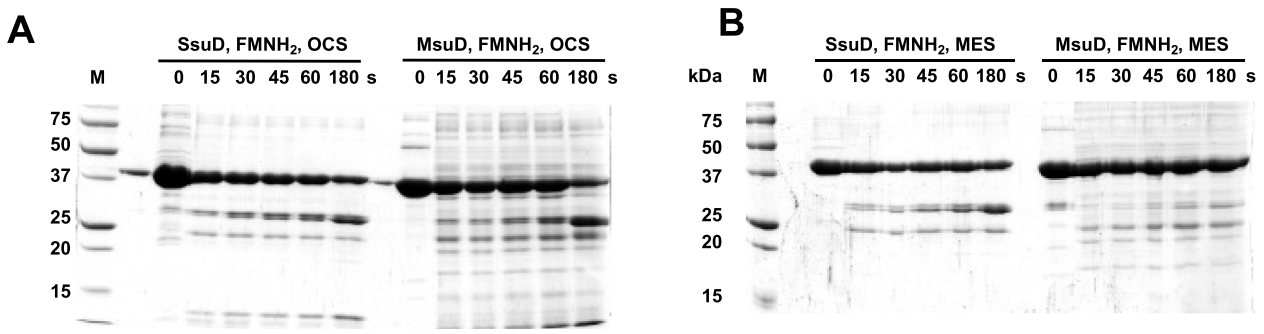

Figure 2. Limited proteolysis of SsuD and MsuD in the presence of $FMNH_2$/OCS and $FMNH_2$/MES. (A) Trypsin digest of SsuD and MsuD with $FMNH_2$ and OCS. (B) Trypsin digest of SsuD and MsuD with $FMNH_2$ and MES. Digestions were performed under anaerobic conditions. Gel lanes: molecular weight marker (M), SsuD and MsuD standard (0 s); aliquots were removed and quenched through heat denaturation after 15, 30, 45, 60, and 180 s.

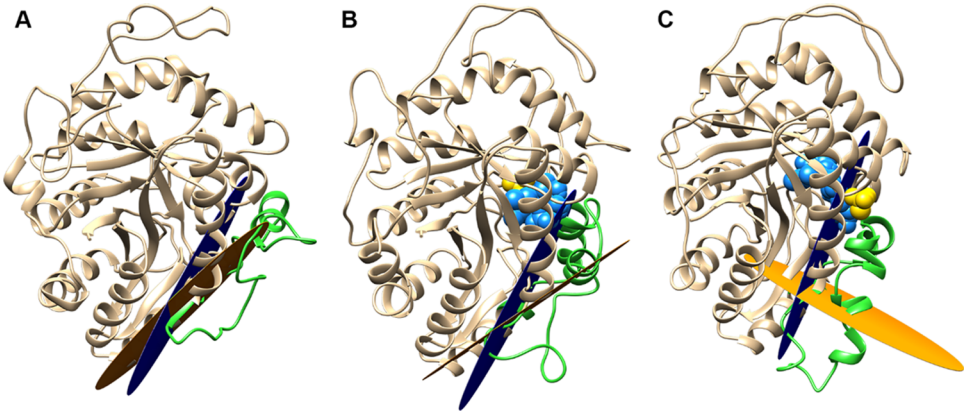

Figure 3. Top cluster structures for (A) MsuD without substrates bound. (B) MsuD/$FMNH_2$/MES. (C) SsuD/$FMNH_2$/MES complexes. The mobile loop plane is colored in orange and the active site entrance plane in dark blue. The flavin (light blue) and MES (yellow) are shown as space filling models.

Table 3. The Top Five Clusters of the MsuD/SsuD Enzyme Complexes and Corresponding Dihedral Angles between the Mobile Loop and the Active Site Plane

	MsuD		MsuD/$FMNH_2$/MES		SsuD/$FMNH_2$/MES	
	occupied %	dih. ang. degree	occupied %	dih. ang. degree	occupied %	dih. ang. degree
cluster 1	44.2	17.2	38.2	28.3	27.1	96.1
cluster 2	9.9	71.3	19.4	32.4	25.7	107.6
cluster 3	9.2	19.6	16.4	30.9	21.3	95.7
cluster 4	8.8	17.9	10.1	33.9	11.3	85.6
cluster 5	6.1	96.1	7.1	25.0	5.3	98.4
total	78.2		91.2		90.7	

Computational Analysis of SsuD and MsuD. *Structural Changes between SsuD and MsuD with $FMNH_2$ and MES.* Clustering analysis was performed on the SsuD and MsuD systems, i.e., apo and bound with substrates, to identify the most prevalent structural configurations over the course of each simulation. Accordingly, the most dominant SsuD and MsuD clusters for each system are illustrated in Figure 3, and their corresponding occupancies are listed in Table 3. The physical similarity of each simulation relative to the initial configuration was investigated using RMSD calculations and indicated that any major conformational changes in MsuD were completed by 200 ns and by 300 ns for SsuD (Figure S6 in the Supporting Information). To computationally investigate the movement of the mobile loop in the $FMNH_2$-dependent monooxygenases with respect to the binding of substrates in the active site, five points near the active site were chosen from the main protein and the mobile loop. The definition of the mobile loop (colored in green in Figure 3), mobile loop plane, and active site plane residues are provided in Table S2 in the Supporting Information. To summarize, the MsuD mobile plane was defined by the α-carbon of Ile245, Gln268, and Leu288 (colored orange in Figure 3), and the second plane that defined the active site entrance was selected by using the α-carbon of Asp110, Ala203, and Leu288 (colored blue in Figure 3). Similarly, the SsuD mobile loop plane was defined by the α-carbon of Ile246, Gln269, and Leu289 and the second plane using the α-carbon of Asp111, Lys204, and Leu289.

A dihedral angle of 17.2 degrees between the mobile loop and active site planes was found for the substrate-free MsuD system that predicted a closed conformation, that is, the mobile loop covered the entrance of the active site for the top

https://doi.org/10.1021/acs.biochem.2c00586
Biochemistry 2023, 62, 85−94

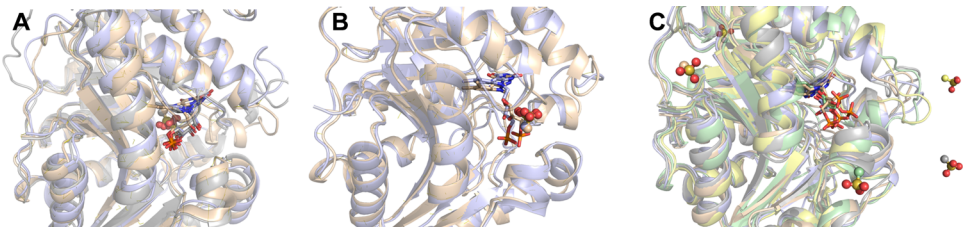

Figure 4. Cluster comparison of the SsuD/$FMNH_2$ structure with MES. (A) Conformation of MES bound at the active site. (B) Conformation of MES bound at the opening of the active site. (C) Conformation of MES bound outside of the active site. The SsuD structures represent overlays of the predominant location of MES from the top 10 clusters shown in Table 4.

cluster configuration with a 44.2% occupancy (Table 3). This differed compared to our previous study of SsuD in which the top cluster for the substrate-free SsuD simulation had a fully open conformation with a dihedral angle of 122.8 degrees with regard to the mobile loop region for 64% of the simulation.[21] Interestingly, when considering dihedral angles of the top five cluster structures of apo MsuD, it was found that the substrate-free enzyme demonstrated increased motion compared to SsuD with the mobile loop/active site plane angles varying between 17.2 and 96.1 degrees (Table 3 and Figure S7 in the Supporting Information). All occupancies and dihedral angles for the top 10 substrate-free MsuD clusters were plotted and are provided in Figure S8 and Table S3 of the Supporting Information. The conformations can be approximately divided into three parts: closed (1st, 3rd, 4th, 6th, and 8th clusters, 73.2% occupancy), semiclosed (2nd, 7th, and 9th clusters, 19.6%), and open (5th and 10th clusters, 7.1%), again emphasizing a very active mobile loop that opens and closes the entrance of the active site over the entire trajectory. However, when the $FMNH_2$ and MES substrates were bound within the active site of the MsuD enzyme, the system behaved more consistently by adopting a closed conformation (~25−34 degree angle between the planes) for the top five clusters that represented 91.2% of the entire simulation (Table 3). Interestingly, the top five clusters of the SsuD/$FMNH_2$/MES system (90.7% of the total frames) had a semiclosed conformation with mobile loop plane dihedral angles between 85.6 and 107.6 degrees. The present SsuD complex with MES was similar in conformation to the previous SsuD study bound with an octanesulfonate substrate (i.e., SsuD/$FMNH_2$/OCS) that also yielded a semiclosed mobile loop conformation of 89.5 degrees.[21]

Comparison of the SsuD Structures with MES and OCS. The aMD analysis of SsuD/$FMNH_2$/MES identified variable clusters due to alterations in the position of MES. The top 10 structures from the clustering analyses of the SsuD/$FMNH_2$/MES complex showed three overall conformations for MES relative to SsuD/$FMNH_2$ (Figure 4): (1) MES at the opening of the active site, (2) bound in the active site, and (3) outside of the active site. MES bound to the opening of the active site was the dominant structure contributing to 52.8% of the total structures, while MES bound at the active site contributed to 33.6% of the clusters (Table 4). Although not as dominant, MES was found at various positions outside of the active site in 13.6% of the structures. Therefore, MES was never stably bound to the active site over the 1000 ns trajectory.

The kinetic analyses of SsuD suggested that the enzyme was unable to catalyze the desulfonation of alkanesulfonates with shorter alkyl chain lengths. An overlay of SsuD/$FMNH_2$/OCS with the SsuD/$FMNH_2$/MES (bound to the active site) clusters shows that $FMNH_2$ has shifted position, but the sulfonate groups of OCS and MES remain in a similar position. For the SsuD/$FMNH_2$/MES complex, there is a restructuring of the active site that leads to an overall shift in $FMNH_2$ compared to the enzyme with $FMNH_2$/OCS bound (Figure 5A). More notable are the variable positions of the MES molecule in the active site of the SsuD/$FMNH_2$/MES clusters

Table 4. The Top 10 Clusters of the SsuD/$FMNH_2$/MES System

cluster	number of frames	fraction		total
1	54,291	0.271	52.8%	the mouth of the pocket
2	51,404	0.257		
3	42,639	0.213	33.6%	the active site position
4	22,548	0.113		
9	1916	0.01		
5	10,673	0.053	13.6%	outside position
6	8603	0.043		
7	3915	0.02		
8	3725	0.019		
10	286	0.001		

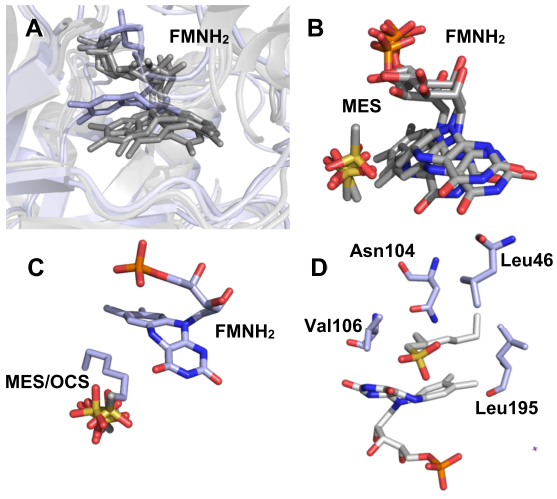

Figure 5. Computational analyses of the active site organization of SsuD with $FMNH_2$ and sulfonate substrates bound. (A) SsuD active site showing a shift in $FMNH_2$ between OCS (blue) and the clusters with MES (gray) bound at the active site. SsuD/$FMNH_2$ complexes with the alkanesulfonate substrates are not shown for clarity. (B) SsuD active site with $FMNH_2$ and MES. SsuD clusters of MES bound at the active site. (C) SsuD active site with OCS (blue) and MES bound clusters. The SsuD/$FMNH_2$/OCS bound structure is overlaid with the clusters of MES bound at the active site. (D) SsuD active site with OCS and $FMNH_2$. The flavin and OCS substrates are highlighted in white. Active site amino acids proposed to stabilize the superoxyanion are highlighted in blue.

https://doi.org/10.1021/acs.biochem.2c00586
Biochemistry 2023, 62, 85−94

(bound in the active site), which suggests that the MES substrate bound in the active site is unstable (Figure 5B). Interestingly, the sulfonate groups of OCS and MES are in a similar position (Figure 5C); however, the repositioning of the active site shifts the flavin N5 in close proximity to C1 of MES leaving limited space for the activation of dioxygen. The alkyl chain of the OCS substrate in the SsuD/$FMNH_2$/OCS complex is packed against the dimethylbenzene portion of the flavin on one side of the alkyl chain and a hydrophobic pocket distal from the active site opening on the other side of the alkyl chain (Figure 5C). This hydrophobic packing is critical in stabilizing the octanesulfonate to properly position the sulfonate group for reaction with the flavin hydroperoxide. One potential reason for the binding instability of MES in the SsuD active site is the slight collapse of the active site in the absence of the alkyl chain. This leads to the observed conformation flexibility of the bound MES in the active site of SsuD leading to the eventual displacement of MES.

RutA is a group C two-component monooxygenase that catalyzes the oxidation of pyrimidine nucleotides and shares similar structural features as SsuD and MsuD.[28] In the O_2-pressurized crystal structure of RutA with oxidized flavin bound, the dioxygen is located within a cavity surrounded by conserved amino acid residues on the *re*-side of the flavin isoalloxazine ring.[29] Several of these amino acids have been proposed to be involved in the binding of dioxygen and stabilization of the superoxyanion.[29] Conversely, the substrate binding site is located on the *si*-side of the isoalloxazine ring. The peroxy group on the N5 is proposed to undergo an inversion from the *re*-side to react with the substrate on the *si*-side of the flavin. Both SsuD and MsuD also share many of these conserved residues for oxygen binding and stabilization of the superoxide.[29] The conserved residues and substrates are both on the *re*-side of the flavin for the SsuD and MsuD structures with $FMNH_2$ and their preferred alkanesulfonate substrate; therefore, a nitrogen inversion would not be necessary to catalyze the desulfonation reaction (Figure 5D).

DISCUSSION

Bacteria are adequately equipped to manage metabolic fluctuations using alternative pathways to maintain their viability. Sulfur is a critical element for the survival of bacteria, and there are alternative mechanisms to ensure that usable forms of sulfur are readily used.[1,2] In some bacteria, both the *msu* and *ssu* operons are expressed together during sulfur limiting conditions to ensure that all available alkanesulfonate substrates can be utilized by the cell.[1,5,6] Sulfonate compounds are produced as intermediates in diverse metabolic pathways and serve as synthetic surfactants in industrial applications. Therefore, these compounds are prevalent in both bacterial hosts and the environment. The two-component $FMNH_2$-dependent alkanesulfonate monooxygenases share a high structural similarity but have a distinct catalytic function.[5,10,29] SsuD showed a clear substrate preference for C4 to C10 alkanesulfonates and was not able to desulfonate methanesulfonate and ethanesulfonate substrates. MsuD showed a broader range of substrate specificity (C1−C10). Even though a broader substrate range was observed, the MsuD enzyme is part of a metabolic pathway that includes the MsuC monooxygenase.[5,30] MsuC catalyzes the oxidation of methanesulfinate to methanesulfonate, and MsuD catalyzes the desulfonation of methanesulfonate to formaldehyde and sulfonate.[10,30] The mechanism for the transfer of methanesulfinate from MsuC to MsuD is not known and could involve complex formation. Therefore, the ability of MsuD to utilize longer alkanesulfonate substrates may not be relevant under physiological conditions when coupled with MsuC.

SsuD could not utilize methanesulfonate as a substrate, but the enzyme had a similar binding affinity for both MES and OCS in the presence of reduced flavin. We had previously shown increased protection from proteolysis for SsuD in the presence of reduced $FMNH_2$ compared to apo SsuD.[11,21] This was attributed to movement of a dynamic loop region over the active site that is part of an insertion sequence that diverges from the classic TIM-barrel structure.[11,21] The loop protection did not change when both $FMNH_2$ and OCS substrates were included with SsuD, and the SsuD/$FMNH_2$ complex with MES showed a similar protection. Previous studies had identified three conformations for SsuD associated with loop closure attributed to substrate binding.[21] The dihedral angle associated with loop closure for the SsuD/$FMNH_2$/MES complex existed in the semiclosed loop conformation as previously observed for the SsuD/$FMNH_2$/OCS complex. MsuD had similar K_d values as SsuD for the binding of both alkanesulfonate substrates (Table 2), and there was increased proteolytic protection seen with the MES and OCS substrates compared to MsuD/$FMNH_2$ (Figure 2). It is interesting that MsuD and SsuD have greater than 60% amino acid sequence identity, but there was a clear difference in the loop conformation with MsuD (Table 3 and Figure 3). The dihedral angle for the MsuD/$FMNH_2$/MES complex was much smaller than the dihedral angle for the comparable SsuD complex, which correlated with the increased proteolytic protection. It has been proposed that the mobile loop may play a role in conveying substrate specificity.[7,10] Although the mobile loop of SsuD and MsuD shows ∼80 amino acid sequence similarity, different conformations of the mobile loop for SsuD and MsuD in the tertiary complex could be important in arranging the active site architecture for alkanesulfonate binding and stabilization. For SsuD and MsuD, the binding of $FMNH_2$ is needed for the preferred alkanesulfonate substrate to bind.[31] Therefore, the binding of reduced flavin must organize the active site for alkanesulfonate binding. Once the alkanesulfonate is bound, a global reorganization of the structure is required for catalytic turnover. Unlike apo SsuD, the mobile loop of apo MsuD showed increased motion compared to SsuD in computational simulations. Under physiological conditions, MsuD would have to accept the methanesulfonate substrate from MsuC and the reduced flavin from MsuE.[10,30] The transfer of $FMNH_2$ from MsuE may be linked to protein−protein interactions, and increased flexibility of MsuD would be important to facilitate protein−protein interactions between multiple partners. Conversely, SsuD does not rely on another enzyme for the sulfonate product, so the flexibility would be limited after the binding of the reduced flavin.

Currently, there are no structures of SsuD with reduced flavin and substrates bound. SsuD/$FMNH_2$ and MES or OCS structures obtained from our computational studies showed a difference in the stability of the bound substrate. The top 10 clusters of SsuD/$FMNH_2$/MES showed that the MES substrate primarily existed at the mouth of the pocket (52.8%), while the clusters with MES bound at the active site made up 33.6% of the total clusters (Table 4). Even when bound to the active site, the MES substrate was not stable and existed in multiple conformations. These results seem

https://doi.org/10.1021/acs.biochem.2c00586
Biochemistry 2023, 62, 85−94

conflicting with the similar affinity observed for SsuD with both MES and OCS. The K_d values were obtained under equilibrium conditions; therefore, a decrease in fluorescence was observed with the addition of MES even though the substrate was not stably bound in computational investigations. The titrations are performed anaerobically to prevent the oxidation of reduced flavin and may not represent the active conformation during catalytic turnover. We had previously proposed that SsuD/$FMNH_2$/OCS may form an inactive complex in the absence of oxygen that undergoes a slow conformational change to an active form in the presence of oxygen.[31] In the comparable structure of SsuD/$FMNH_2$/OCS, the alkane chain of OCS is stabilized in a hydrophobic pocket that places the sulfonate substrate near the N5 of the flavin. The lack of a long alkyl chain with the MES substrate prevents the stabilization and leads to a collapse of the flavin and a restructuring of the active site, which explains the observed protection seen in proteolytic studies. Activity is not observed for SsuD with the alkanesulfonate substrates until a chain length of C4 is reached providing a chain length conducive to hydrophobic stabilization. The sulfonate group likely contributes to initial substrate recognition, but the alkyl chain length plays a critical role in stabilizing the binding of alkanesulfonate in SsuD. Previous structural work to evaluate substrate binding with MsuD was with the oxidized flavin product alone or with the MES substrate.[10] There is a 100-fold increase in the binding affinity for FMN compared to reduced flavin for both SsuD and MsuD (Table 2). Therefore, conformational changes may lead to alterations in the binding specificity for a specific redox form of the flavin. Structural investigations into the binding specificity for both SsuD and MsuD should be performed with both the $FMNH_2$ substrate and FMN to detect subtle conformational changes. For the three-dimensional structure of the MsuD/FMN/MES complex, both the mobile loop and the C-terminal end of the enzyme played a role in alkanesulfonate specificity with the oxidized flavin product.[10] The C-terminal end of the enzyme formed intersubunit hydrogen bonds with an adjacent subunit. Similar interactions with the reduced flavin substrate were not observed in these studies as the simulations were performed with a single subunit. An unexpected result from these studies was the difference in reduced flavin binding between the three-dimensional crystal structure of MsuD with FMN/MES and the computational investigations with $FMNH_2$ and MES. There were increased contacts made with the phosphate group in the MsuD/$FMNH_2$/MES complex. The binding site around the phosphate makes additional electrostatic and hydrogen-bonding contacts in the MsuD/$FMNH_2$/MES complex that would lead to the increased binding affinity observed with reduced flavin compared to oxidized flavin.

The activation of dioxygen by several two-component monooxygenase enzymes has been proposed to occur through the formation of a flavin N5 oxygenating intermediate.[29,32−39] An N5-oxide is often formed as an intermediate in the reaction or as a final product. For the group C two-component monooxygenase YxeK, the enzyme utilizes an N5-peroxyflavin to salvage *S*-(2-succino)cysteine; however, a stable N5-oxide intermediate is not observed.[39] Similar to YxeK, a flavin N5 has been proposed to facilitate electron transfer from the isoalloxazine ring to oxygen to form a superoxide intermediate for both SsuD and MsuD.[10,29,39] The superoxide is stabilized by conserved polar amino acids to promote radical coupling between the superoxide radical and the N5 position of the isoalloxazine ring of the flavin to form the N5-(hydro)-peroxyflavin. Three-dimensional structures of two-component monooxygenases with bound substrates showed a delineation between the oxygen activation site and the site of substrate oxidation.[29,39] It was proposed that an N5 inversion would need to occur to move the N5-peroxyflavin to the substrate binding site for oxidation. The MsuD and SsuD structures with $FMNH_2$ and alkanesulfonates bound do not show a defined separation between the proposed oxygen activation and substrate oxidation sites. The reduced flavin observed in computational structures had moved relative to the oxidized flavin to allow sequential oxidation, which was not dependent on a spatial separation. Therefore, the N5-peroxyflavin would not need to undergo an inversion to react with the alkane sulfonated substrate in the computational models. Given the differences in binding affinity between the different redox forms of the flavin for some two-component monooxygenases, structural analyses of both the oxidized and reduced forms of the flavin will need to be performed.

■ ASSOCIATED CONTENT

Supporting Information

The Supporting Information is available free of charge at https://pubs.acs.org/doi/10.1021/acs.biochem.2c00586.

Protein sequence; boost parameter aMD simulations; kinetic plots; titration plots; SDS-PAGE gel; RMSD; cluster structures of MsuD; MsuD cluster occupancy % (PDF)

Accession Codes

SsuE (UniProt entry: P80644); SsuD (UniProt entry: P80645); MsuE (UniProt entry: Q88J85); MsuD (UniProt entry: Q9I1C2).

■ AUTHOR INFORMATION

Corresponding Author

Holly R. Ellis − *Department of Biochemistry and Molecular Biology, Brody School of Medicine at East Carolina University, Greenville, North Carolina 27834, United States;* orcid.org/0000-0003-0521-422X; Email: ellish20@ecu.edu

Authors

Shruti Somai − *Department of Biochemistry and Molecular Biology, Brody School of Medicine at East Carolina University, Greenville, North Carolina 27834, United States*

Kun Yue − *Department of Chemistry, University of Miami, Coral Gables, Florida 33146, United States*

Orlando Acevedo − *Department of Chemistry, University of Miami, Coral Gables, Florida 33146, United States;* orcid.org/0000-0002-6110-3930

Complete contact information is available at: https://pubs.acs.org/10.1021/acs.biochem.2c00586

Author Contributions

[§]S.S. and K.Y. contributed equally to this work.

Notes

The authors declare no competing financial interest.

■ ACKNOWLEDGMENTS

Gratitude is expressed to the National Science Foundation (CHE-1808495 and 2105998) and the University of Miami

Institute for Data Science and Computing for support of this research.

REFERENCES

(1) Kertesz, M. A. Riding the sulfur cycle–metabolism of sulfonates and sulfate esters in gram-negative bacteria. *FEMS Microbiol. Rev.* **2000**, *24*, 135−175.

(2) Kertesz, M. A.; Wietek, C. Desulfurization and desulfonation: applications of sulfur-controlled gene expression in bacteria. *Appl. Microbiol. Biotechnol.* **2001**, *57*, 460−466.

(3) Kertesz, M. A.; Leisinger, T.; Cook, A. M. Proteins induced by sulfate limitation in *Escherichia coli*, *Pseudomonas putida*, or *Staphylococcus aureus*. *J. Bacteriol.* **1993**, *175*, 1187−1190.

(4) Kertesz, M. A. Desulfonation of aliphatic sulfonates by *Pseudomonas aeruginosa* PAO. *FEMS Microbiol. Lett.* **1996**, *137*, 221−225.

(5) Kertesz, M. A.; Schmidt-Larbig, K.; Wüest, T. A novel reduced flavin mononucleotide-dependent methanesulfonate sulfonatase encoded by the sulfur-regulated msu operon of *Pseudomonas aeruginosa*. *J. Bacteriol.* **1999**, *181*, 1464−1473.

(6) Tralau, T.; Vuilleumier, S.; Thibault, C.; Campbell, B. J.; Hart, C. A.; Kertesz, M. A. Transcriptomic analysis of the sulfate starvation response of *Pseudomonas aeruginosa*. *J. Bacteriol.* **2007**, *189*, 6743−6750.

(7) Ellis, H. R. The FMN-dependent two-component monooxygenase systems. *Arch. Biochem. Biophys.* **2010**, *497*, 1−12.

(8) Huijbers, M. M. E.; Montersino, S.; Westphal, A. H.; Tischler, D.; van Berkel, W. J. H. Flavin dependent monooxygenases. *Arch. Biochem. Biophys.* **2014**, *544*, 2−17.

(9) Eichhorn, E.; Davey, C. A.; Sargent, D. F.; Leisinger, T.; Richmond, T. J. Crystal structure of *Escherichia coli* alkanesulfonate monooxygenase SsuD. *J. Mol. Biol.* **2002**, *324*, 457−468.

(10) Liew, J. J. M.; El Saudi, I. M.; Nguyen, S. V.; Wicht, D. K.; Dowling, D. P. Structures of the alkanesulfonate monooxygenase MsuD provide insight into C-S bond cleavage, substrate scope, and an unexpected role for the tetramer. *J Biol Chem* **2021**, *297*, No. 100823.

(11) Carpenter, R. A.; Xiong, J.; Robbins, J. M.; Ellis, H. R. Functional role of a conserved arginine residue located on a mobile loop of alkanesulfonate monooxygenase. *Biochemistry* **2011**, *50*, 6469−6477.

(12) Wierenga, R. K. The TIM-barrel fold: a versatile framework for efficient enzymes. *FEBS Lett.* **2001**, *492*, 193−198.

(13) Malabanan, M. M.; Amyes, T. L.; Richard, J. P. A role for flexible loops in enzyme catalysis. *Curr. Opin. Struct. Biol.* **2010**, *20*, 702−710.

(14) Xiong, J.; Ellis, H. R. Deletional studies to investigate the functional role of a dynamic loop region of alkanesulfonate monooxygenase. *Biochim. Biophys. Acta* **2012**, *1824*, 898−906.

(15) Jumper, J.; Evans, R.; Pritzel, A.; Green, T.; Figurnov, M.; Ronneberger, O.; Tunyasuvunakool, K.; Bates, R.; Žídek, A.; Potapenko, A.; Bridgland, A.; Meyer, C.; Kohl, S. A. A.; Ballard, A. J.; Cowie, A.; Romera-Paredes, B.; Nikolov, S.; Jain, R.; Adler, J.; Back, T.; Petersen, S.; Reiman, D.; Clancy, E.; Zielinski, M.; Steinegger, M.; Pacholska, M.; Berghammer, T.; Bodenstein, S.; Silver, D.; Vinyals, O.; Senior, A. W.; Kavukcuoglu, K.; Kohli, P.; Hassabis, D. Highly accurate protein structure prediction with AlphaFold. *Nature* **2021**, *596*, 583−589.

(16) Eichhorn, E.; van der Ploeg, J. R.; Leisinger, T. Characterization of a two-component alkanesulfonate monooxygenase from *Escherichia coli*. *J Biol Chem* **1999**, *274*, 26639−26646.

(17) Gao, B.; Ellis, H. R. Altered mechanism of the alkanesulfonate FMN reductase with the monooxygenase enzyme. *Biochem. Biophys. Res. Commun.* **2005**, *331*, 1137−1145.

(18) McFarlane, J. S.; Hagen, R. A.; Chilton, A. S.; Forbes, D. L.; Lamb, A. L.; Ellis, H. R. Not as easy as π: An insertional residue does not explain the π-helix gain-of-function in two-component FMN reductases. *Protein Sci.* **2019**, *28*, 123−134.

(19) Hamelberg, D.; Mongan, J.; McCammon, J. A. Accelerated molecular dynamics: a promising and efficient simulation method for biomolecules. *J Chem Phys* **2004**, *120*, 11919−11929.

(20) Pierce, L. C.; Salomon-Ferrer, R.; Augusto F de Oliveira, C.; McCammon, J. A.; Walker, R. C. Routine Access to Millisecond Time Scale Events with Accelerated Molecular Dynamics. *J. Chem. Theory Comput.* **2012**, *8*, 2997−3002.

(21) Thakur, A.; Somai, S.; Yue, K.; Ippolito, N.; Pagan, D.; Xiong, J.; Ellis, H. R.; Acevedo, O. Substrate-Dependent Mobile Loop Conformational Changes in Alkanesulfonate Monooxygenase from Accelerated Molecular Dynamics. *Biochemistry* **2020**, *59*, 3582−3593.

(22) Salomon-Ferrer, R.; Götz, A. W.; Poole, D.; Le Grand, S.; Walker, R. C. Routine Microsecond Molecular Dynamics Simulations with AMBER on GPUs. 2. Explicit Solvent Particle Mesh Ewald. *J. Chem. Theory Comput.* **2013**, *9*, 3878−3888.

(23) Jorgensen, W. L.; Chandrasekhar, J.; Madura, J. D.; Impey, R. W.; Klein, M. L. Comparison of simple potential functions for simulating liquid water. *J. Chem. Phys.* **1983**, 926.

(24) Wickstrom, L.; Okur, A.; Simmerling, C. Evaluating the performance of the ff99SB force field based on NMR scalar coupling data. *Biophys. J.* **2009**, *97*, 853−856.

(25) Wang, J.; Wolf, R. M.; Caldwell, J. W.; Kollman, P. A.; Case, D. A. Development and testing of a general amber force field. *J. Comput. Chem.* **2004**, *25*, 1157−1174.

(26) Gedeon, P. C.; Thomas, J. R.; Madura, J. D. Accelerated molecular dynamics and protein conformational change: a theoretical and practical guide using a membrane embedded model neurotransmitter transporter. *Methods Mol. Biol.* **2015**, *1215*, 253−287.

(27) Roe, D. R.; Cheatham, T. E., III PTRAJ and CPPTRAJ: Software for Processing and Analysis of Molecular Dynamics Trajectory Data. *J. Chem. Theory Comput.* **2013**, *9*, 3084−3095.

(28) Mukherjee, T.; Zhang, Y.; Abdelwahed, S.; Ealick, S. E.; Begley, T. P. Catalysis of a flavoenzyme-mediated amide hydrolysis. *J. Am. Chem. Soc.* **2010**, *132*, 5550−5551.

(29) Matthews, A.; Saleem-Batcha, R.; Sanders, J. N.; Stull, F.; Houk, K. N.; Teufel, R. Aminoperoxide adducts expand the catalytic repertoire of flavin monooxygenases. *Nat. Chem. Biol.* **2020**, *16*, 556−563.

(30) Soule, J.; Gnann, A. D.; Gonzalez, R.; Parker, M. J.; McKenna, K. C.; Nguyen, S. V.; Phan, N. T.; Wicht, D. K.; Dowling, D. P. Structure and function of the two-component flavin-dependent methanesulfinate monooxygenase within bacterial sulfur assimilation. *Biochem. Biophys. Res. Commun.* **2020**, *522*, 107−112.

(31) Zhan, X.; Carpenter, R. A.; Ellis, H. R. Catalytic importance of the substrate binding order for the $FMNH_2$-dependent alkanesulfonate monooxygenase enzyme. *Biochemistry* **2008**, *47*, 2221−2230.

(32) Teufel, R.; Miyanaga, A.; Michaudel, Q.; Stull, F.; Louie, G.; Noel, J. P.; Baran, P. S.; Palfey, B.; Moore, B. S. Flavin-mediated dual oxidation controls an enzymatic Favorskii-type rearrangement. *Nature* **2013**, *503*, 552−556.

(33) Teufel, R.; Stull, F.; Meehan, M. J.; Michaudel, Q.; Dorrestein, P. C.; Palfey, B.; Moore, B. S. Biochemical Establishment and Characterization of EncM's Flavin-N5-oxide Cofactor. *J. Am. Chem. Soc.* **2015**, *137*, 8078−8085.

(34) Teufel, R. Preparation and Characterization of the Favorskiiase Flavoprotein EncM and Its Distinctive Flavin-N5-Oxide Cofactor. *Methods Enzymol.* **2018**, *604*, 523−540.

(35) Adak, S.; Begley, T. P. Dibenzothiophene Catabolism Proceeds via a Flavin-N5-oxide Intermediate. *J. Am. Chem. Soc.* **2016**, *138*, 6424−6426.

(36) Adak, S.; Begley, T. P. Flavin-N5-oxide: A new, catalytic motif in flavoenzymology. *Arch. Biochem. Biophys.* **2017**, *632*, 4−10.

(37) Adak, S.; Begley, T. P. RutA-Catalyzed Oxidative Cleavage of the Uracil Amide Involves Formation of a Flavin-N5-oxide. *Biochemistry* **2017**, *56*, 3708−3709.

(38) Adak, S.; Begley, T. P. Flavin-N5-oxide intermediates in dibenzothiophene, uracil, and hexachlorobenzene catabolism. *Methods Enzymol.* **2019**, *620*, 455−468.

https://doi.org/10.1021/acs.biochem.2c00586
Biochemistry 2023, 62, 85−94

(39) Matthews, A.; Schönfelder, J.; Lagies, S.; Schleicher, E.; Kammerer, B.; Ellis, H. R.; Stull, F.; Teufel, R. Bacterial flavoprotein monooxygenase YxeK salvages toxic S-(2-succino)-adducts via oxygenolytic C-S bond cleavage. *FEBS J.* **2022**, *289*, 787−807.

https://doi.org/10.1021/acs.biochem.2c00586
Biochemistry 2023, 62, 85−94